

# Polarization observables and spin-aligned fusion rates in ${}^2\text{H}(d,p){}^3\text{H}$ and ${}^2\text{H}(d,n){}^3\text{He}$ reactions

A. Deltuva\* and A. C. Fonseca

*Centro de Física Nuclear da Universidade de Lisboa, P-1649-003 Lisboa, Portugal*

(Received February 24, 2010)

Nucleon transfer reactions in low-energy deuteron-deuteron scattering are described by solving exact four-particle equations in momentum space. The Coulomb interaction between the protons is included using the screening and renormalization method. Various realistic potentials are used between nucleon pairs. The energy dependence of the differential cross section, analyzing powers, polarizations, spin-transfer coefficient, and the quintet suppression factor is studied.

PACS numbers: 21.30.-x, 21.45.-v, 24.70.+s, 25.10.+s

Neutron ( $n$ ) and proton ( $p$ ) transfer reactions in deuteron-deuteron ( $d$ - $d$ ) scattering,  $d + d \rightarrow p + {}^3\text{H}$  and  $d + d \rightarrow n + {}^3\text{He}$ , are amongst the simplest nuclear reactions where charge-symmetry breaking (CSB) in the nuclear force can be verified or searched for. For that purpose one needs a very precise calculation of the four-nucleon ( $4N$ ) problem with different interaction models based on nucleon-nucleon ( $NN$ ) and many-nucleon forces together with the inclusion of the Coulomb force between protons which is the most important cause of CSB. Such task is now possible in view of the progress achieved in the past few years [1, 2] on the solution of exact Alt, Grassberger, and Sandhas (AGS) equations [3] for four-particle transitions operators that, in addition to the strong nuclear force, include also the Coulomb interaction.

The aim of the present paper is to study the energy dependence of the  $d + d \rightarrow p + {}^3\text{H}$  and  $d + d \rightarrow n + {}^3\text{He}$  observables below three-body breakup threshold using different nuclear force models. In addition to the differential cross sections [4–7] there are precise measurements of the deuteron analyzing powers between 1.5 and 4 MeV deuteron lab energy [6, 8]. The analyzing powers show a complex structure of maxima and minima that in some cases varies rapidly with the energy. These rapid variations and complex structure means that different  $dd$  partial waves play a significant role, and agreement or disagreement with experimental data at different energies may result from a delicate interplay between them. The contribution of each partial wave to the observables and their evolution with the energy is analyzed.

Other observables that were measured but never analyzed through exact  $4N$  calculations are polarization of the outgoing nucleon [9] and deuteron to nucleon spin transfer coefficients [10, 11]; they are also calculated in the present work.

Furthermore, we will get back to an old issue that remains of interest to  $d$ - $d$  fusion in hot plasma. It was initially believed [12] that at very low energy the production of neutrons resulting from  $d + d \rightarrow n + {}^3\text{He}$  could be controlled by polarizing all deuterons in the plasma such that

only spin-aligned  $d$ - $d$  fusion would take place. If spin-aligned  $d + d \rightarrow n + {}^3\text{He}$  reaction would be significantly suppressed compared to  $d + d \rightarrow p + {}^3\text{H}$ , one would have a significant reduction of undesired neutrons coming out of the plasma. In the past many approximate calculations were made that yielded contradicting results. More sophisticated calculations [13] indicated that no strong suppression should be expected. The present well-converged  $4N$  calculations aim at settling the assumption on the possible suppression of  $d + d \rightarrow n + {}^3\text{He}$  reaction with spin-aligned deuterons.

Our description of the  $4N$  system is based on exact four-particle equations for the transition operators as derived by Alt, Grassberger, and Sandhas [3]; they are equivalent to the Faddeev-Yakubovsky equations [14] for the wave-function components. Since in the isospin formalism protons and neutrons can be considered as identical particles, the symmetrized form of the AGS equations [1, 2] is appropriate. Although the initial  $d$ - $d$  state has total isospin  $\mathcal{T} = 0$ , the final  $n$ - ${}^3\text{He}$  and  $p$ - ${}^3\text{H}$  states are dominated by both isospin  $\mathcal{T} = 0$  and  $\mathcal{T} = 1$  components; a very small admixture of  $\mathcal{T} = 2$  is present due to the charge dependence of the hadronic and electromagnetic interactions. The most important source for the total isospin nonconservation is the Coulomb force between the protons; it is included using the method of screening and renormalization [15–18]. The hadronic charge dependence, as given by the modern  $NN$  potentials, is taken into account as well. After partial wave decomposition, the AGS equations are a system of three-variable integral equations that are solved numerically without any approximation beyond the usual discretization of momentum variables on a finite mesh; technical details are given in Refs. [1, 2]. The results we present are well converged with respect to the partial-wave expansion, the number of momentum meshpoints, and the Coulomb screening radius used to calculate the short-range part of the amplitudes. In this way the discrepancies with the experimental data may be attributed solely to the underlying  $NN$  forces or lack of many-nucleon forces.

As two-nucleon interactions we use the phenomenological potentials Argonne V18 (AV18, hadronic part only) [19], charge-dependent Bonn (CD Bonn) [20], and

---

\* deltuva@cii.fc.ul.pt

inside nonlocal outside Yukawa (INOY04) potential by Doleschall [21], and the one derived from the chiral perturbation theory at next-to-next-to-next-to-leading order (N3LO) [22]. Furthermore, we consider also a two-baryon coupled-channel potential including virtual excitation of a nucleon to a  $\Delta$  isobar [23] that in the  $4N$  system yields effective  $3N$  and  $4N$  forces [24]. Point Coulomb is added for  $pp$  pairs.  ${}^3\text{He}$  and  ${}^3\text{H}$  binding energies calculated with those potentials are collected in the Table I. Thus, the presence of the  $3N$  force is also simulated by the potential INOY04 that fits both  ${}^3\text{He}$  and  ${}^3\text{H}$  experimental binding energies and thereby of all the used potentials is the only one that reproduces correctly the momenta of the final  $n$ - ${}^3\text{He}$  and  $p$ - ${}^3\text{H}$  states. For this reason it is not surprising to see that INOY04 potential gives the best description of  $d+d \rightarrow n+{}^3\text{He}$  and  $d+d \rightarrow p+{}^3\text{H}$  data. We therefore show the predictions of all potentials for the reactions at deuteron lab energy  $E_d = 3$  MeV but study the energy dependence of the observables using INOY04 only.

	$B({}^3\text{H})$	$B({}^3\text{He})$	$P_D(d)$
AV18	7.66	6.95	5.78
N3LO	7.85	7.13	4.51
CD Bonn	8.00	7.26	4.85
CD Bonn + $\Delta$	8.28	7.53	4.85
INOY04	8.49	7.73	3.60
Experiment	8.48	7.72	

TABLE I.  ${}^3\text{H}$  and  ${}^3\text{He}$  binding energies (in MeV) and deuteron  $D$ -state probability  $P_D(d)$  (in percent) for different  $NN$  potentials.

Although  $d$ - $d$  elastic scattering is calculated simultaneously with the transfer reactions, it is a less interesting case and therefore not discussed in the present work: As demonstrated in Refs. [2, 24], the  $d$ - $d$  elastic cross section data is well described by all  $NN$  force models and the corresponding deuteron analyzing powers are very small with quite large error bars that preclude physics conclusions.

In Fig. 1 we present the differential cross section  $d\sigma/d\Omega$  results for both  $d+d \rightarrow p+{}^3\text{H}$  and  $d+d \rightarrow n+{}^3\text{He}$  reactions at  $E_D = 1.5, 3,$  and  $4$  MeV as function of the nucleon center-of-mass (c.m.) scattering angle  $\Theta_{\text{c.m.}}$ . This observable is symmetric with respect to  $\Theta_{\text{c.m.}} = 90^\circ$ . While at the lowest energy the differential cross section is flat between  $\Theta_{\text{c.m.}} = 60^\circ$  and  $120^\circ$ , with increasing energy it develops a minima around  $\Theta_{\text{c.m.}} = 55^\circ$  and  $125^\circ$  and a local maximum at  $\Theta_{\text{c.m.}} = 90^\circ$ . Furthermore,  $d\sigma/d\Omega$  increases with energy at forward and backward angles. There is a good agreement between the experimental data and the predictions of the INOY04 potential whereas other models overestimate the data, especially at forward and backward angles; furthermore, the discrepancy seems to be proportional to the defect in theoretical  ${}^3\text{He}$  and  ${}^3\text{H}$  binding energies. Thus, the differential cross section in the considered transfer reactions corre-

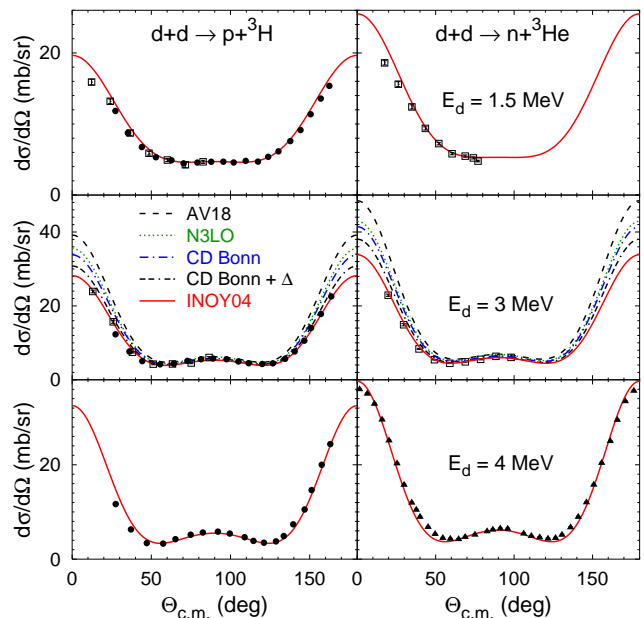


FIG. 1. (Color online) Differential cross section of  $d+d \rightarrow p+{}^3\text{H}$  and  $d+d \rightarrow n+{}^3\text{He}$  reactions at 1.5, 3, and 4 MeV deuteron lab energy as function of the nucleon c.m. scattering angle. Results obtained with various realistic  $NN$  potentials are compared with the experimental data from Refs. [4] (squares), [6, 7] (circles), and [5] (triangles); the latter set is taken at  $E_d = 3.7$  MeV.

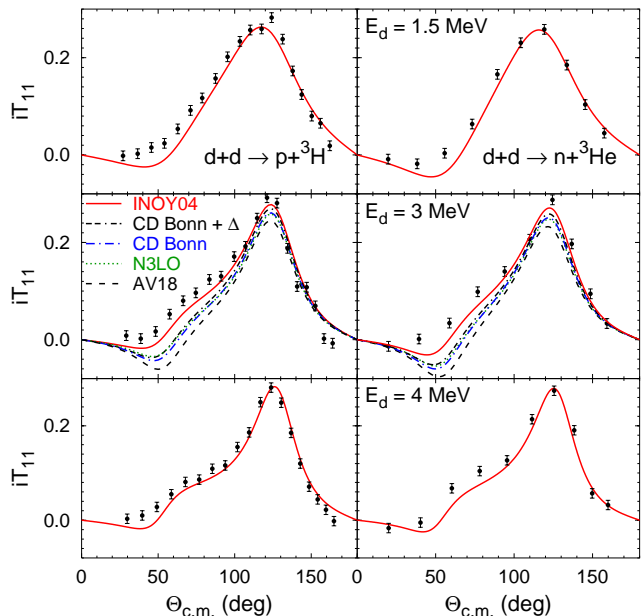


FIG. 2. (Color online) Deuteron vector analyzing power  $iT_{11}$  of  $d+d \rightarrow p+{}^3\text{H}$  and  $d+d \rightarrow n+{}^3\text{He}$  reactions at 1.5, 3, and 4 MeV deuteron lab energy. The data are from Ref. [6, 7] for  $d+d \rightarrow p+{}^3\text{H}$  and from Ref. [8] for  $d+d \rightarrow n+{}^3\text{He}$ .

lates nearly linearly with  $3N$  binding energies.

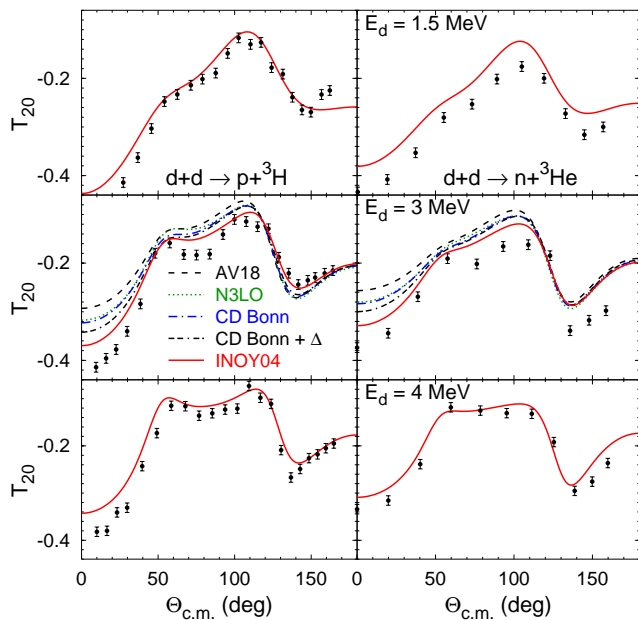


FIG. 3. (Color online) Same as Fig. 2 but for the deuteron tensor analyzing power  $T_{20}$ .

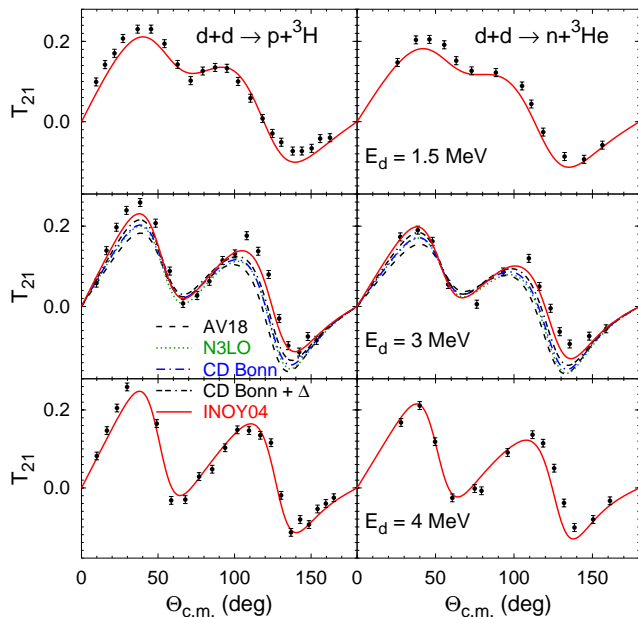


FIG. 4. (Color online) Same as Fig. 2 but for the deuteron tensor analyzing power  $T_{21}$ .

In Figs. 2 - 5 we present the corresponding results for the deuteron analyzing powers. The vector analyzing power  $iT_{11}$  in Fig. 2 varies quite slowly with the energy. The experimental data are well reproduced by the INOY04 model, although a small discrepancy remains around  $\Theta_{c.m.} = 45^\circ$ . More significant discrepancies take place in the tensor analyzing power  $T_{20}$  (Fig. 3) at small

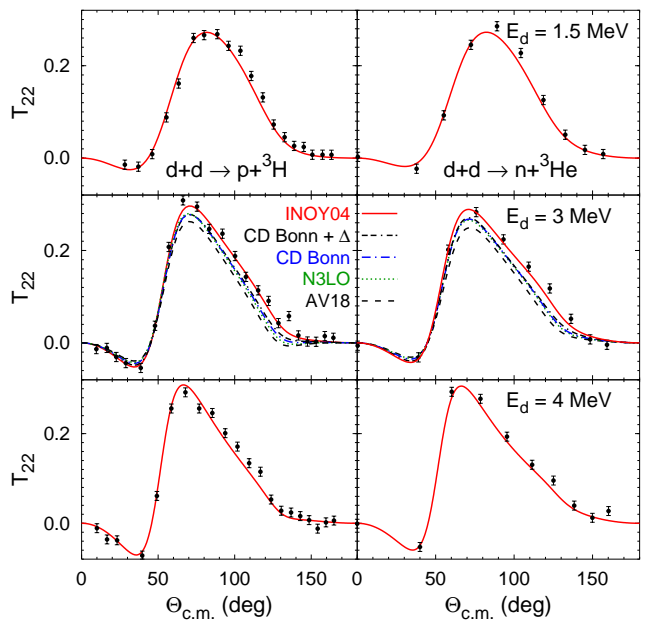


FIG. 5. (Color online) Same as Fig. 2 but for the deuteron tensor analyzing power  $T_{22}$ .

scattering angles, although this observable is slightly overestimated almost in the whole kinematical regime. Nevertheless, the energy dependence of  $T_{20}$ , being considerably stronger than for  $iT_{11}$ , is well reproduced by the calculations. The tensor analyzing power  $T_{21}$  (Fig. 4), though showing strong energy dependence at intermediate angles, is quite well accounted for by the INOY04 predictions. The description of the tensor analyzing power  $T_{22}$  (Fig. 5) is even better; this observable, much like  $iT_{11}$ , varies slowly with the energy. The results obtained with other  $NN$  potentials at  $E_d = 3$  MeV deviate from the respective data more significantly. Furthermore, even if the reproduction of experimental binding energies is an important factor, it is certainly not the only one that matters since the linear correlation with  $3N$  binding energies seems to be violated, e.g., for  $iT_{11}$  at  $\Theta_{c.m.}$  between  $40^\circ$  and  $90^\circ$ , or for  $T_{22}$  between  $\Theta_{c.m.} = 60^\circ$  and  $120^\circ$ , the predictions of N3LO, CD Bonn, and CD Bonn +  $\Delta$  almost coincide despite quite significant differences (up to 0.4 MeV) in the respective  $3N$  binding energies while the predictions of INOY04 and AV18 stay well separated. A closer look into the calculated properties of deuteron,  ${}^3\text{He}$ , and  ${}^3\text{H}$  as given in Table I suggests that the considered spin observables correlate, in addition to the  $3N$  binding energy, also with the  $D$ -state probability of deuteron  $P_D(d)$ . The correlation between  $P_D(d)$  and  $3N$  binding energy takes place for most phenomenological  $NN$  potentials, but N3LO and CD Bonn +  $\Delta$  models clearly violate that correlation thereby allowing to study the dependence of  $4N$  observables on both  $3N$  binding energy and  $P_D(d)$ . The results in Figs. 2 - 5 indicate that increasing the  $3N$  binding energy and decreasing

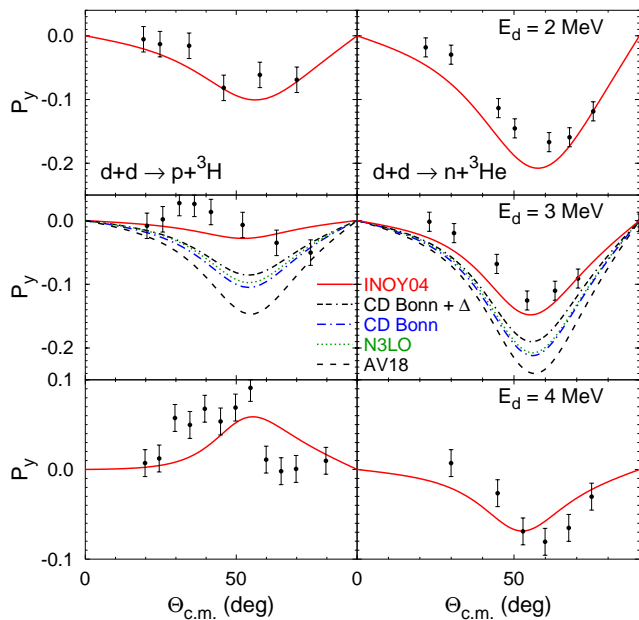


FIG. 6. (Color online) Outgoing nucleon polarization  $P_y$  of  $d + d \rightarrow p + {}^3\text{H}$  and  $d + d \rightarrow n + {}^3\text{He}$  reactions at 2, 3, and 4 MeV deuteron lab energy. The data are from Ref. [9].

$P_D(d)$  move the theoretical predictions into the same direction but the corresponding rates, i.e., strength of the correlations, depend on the observable and kinematical regime. One may conjecture that by a slight decrease of  $P_D(d)$  of INOY04 while keeping the  ${}^3\text{He}$  and  ${}^3\text{H}$  binding energies unchanged one might be able to cure the  $iT_{11}$  discrepancy around  $\Theta_{\text{c.m.}} = 45^\circ$ . However,  $T_{20}$  shows quite weak correlation with  $P_D(d)$  and therefore its description would not be improved significantly by a small decrease of  $P_D(d)$ .

In Fig. 6 we present the results for the polarization  $P_y$  of the outgoing nucleon in  $d + d \rightarrow p + {}^3\text{H}$  and  $d + d \rightarrow n + {}^3\text{He}$  reactions; this observable is equivalent to the nucleon analyzing power  $A_y$  in the time-reverse reactions  $p + {}^3\text{H} \rightarrow d + d$  and  $n + {}^3\text{He} \rightarrow d + d$ .  $P_y$  is antisymmetric with respect to  $\Theta_{\text{c.m.}} = 90^\circ$ ; we therefore show only the angular regime up to  $\Theta_{\text{c.m.}} = 90^\circ$  that contains all the available data.  $P_y$  shows quite strong energy dependence; in the  $d + d \rightarrow p + {}^3\text{H}$  case it even changes the sign when  $E_d$  varies from 2 MeV to 4 MeV being almost zero at  $E_d = 3$  MeV. In the  $d + d \rightarrow n + {}^3\text{He}$  case the observable changes with the same trend but with about 1.5 MeV shift in the energy. The qualitative reproduction of the experimental data having large errorbars is quite successful by the potential INOY04 whereas predictions of the other interaction models are further away. As the deuteron analyzing powers, the nucleon polarization correlates not only with the  $3N$  binding energy but also with  $P_D(d)$  as one can see by comparing N3LO, CD Bonn, and CD Bonn +  $\Delta$  results.

Next we consider double polarization observables for

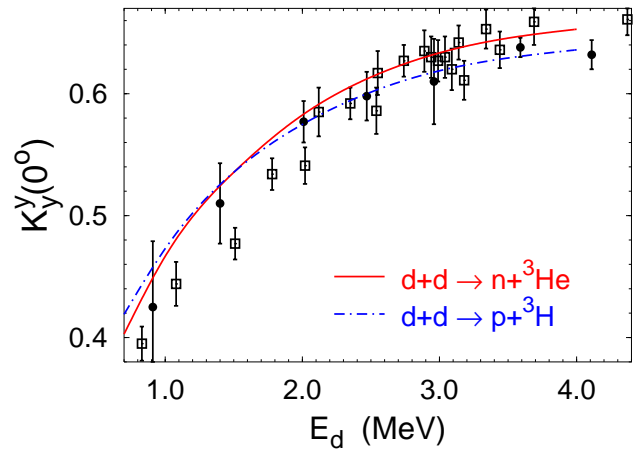


FIG. 7. (Color online) Deuteron to nucleon spin transfer coefficient  $K_y^y$  for  $d + d \rightarrow p + {}^3\text{H}$  and  $d + d \rightarrow n + {}^3\text{He}$  reactions at  $\Theta_{\text{c.m.}} = 0^\circ$  as function of the deuteron lab energy. The data are from Ref. [10] (circles) and from Ref. [11] (squares); both sets refer to the  $d + d \rightarrow n + {}^3\text{He}$  reaction.

which, unfortunately, the experimental data are much scarcer. The deuteron to neutron spin transfer coefficient  $K_y^y$  has been measured in several experiments [10, 11], however, only for the neutrons emitted in the forward direction  $\Theta_{\text{c.m.}} = 0^\circ$ ; the data for the corresponding observable in the  $d + d \rightarrow p + {}^3\text{H}$  reaction is not available below the three-body breakup threshold. In Fig. 7 we compare the deuteron to neutron spin transfer coefficient  $K_y^y(0^\circ)$  calculated using the INOY04 potential with two sets of experimental data in the energy range  $0.75 \leq E_d \leq 4$  MeV. There is a good agreement above  $E_d = 2$  MeV while at lower energies, where the observable shows stronger energy dependence, the data points from Ref. [11] are slightly overpredicted. We include in Fig. 7 also the calculated  $K_y^y(0^\circ)$  for the  $d + d \rightarrow p + {}^3\text{H}$  reaction that shows a similar behavior. The dependence on the  $NN$  force model is quite weak for  $K_y^y(0^\circ)$ , considerably smaller than the experimental error bars: at  $E_d = 3$  MeV the predictions of AV18, N3LO, CD Bonn, CD Bonn +  $\Delta$ , and INOY04 are 0.622, 0.626, 0.630, 0.632, and 0.633, respectively.

In Fig. 8 we study the contribution of various initial and final state partial waves characterized by the relative two-cluster, i.e.,  $d-d$ ,  $n-{}^3\text{He}$ , and  $p-{}^3\text{H}$ , orbital angular momentum  $L$ . Since  $d + d \rightarrow p + {}^3\text{H}$  and  $d + d \rightarrow n + {}^3\text{He}$  observables show similar behavior, we restrict our study to the latter reaction at  $E_d = 1.5$  and 4 MeV. We performed a series of calculations with INOY04 potential including  $L \leq L_{\text{max}}$  with  $L_{\text{max}}$  ranging from 1 to 5. The predictions with  $L_{\text{max}} = 4$  and 5 are very close, indicating that the  $L = 5$  contribution is very small; however, since the convergence is not monotonic, we have also verified that  $L = 6$  contribution can be safely neglected. In contrast, the partial waves with  $L = 4$  yield a sizable contribution at  $E_d = 4$  MeV and for the deuteron ten-

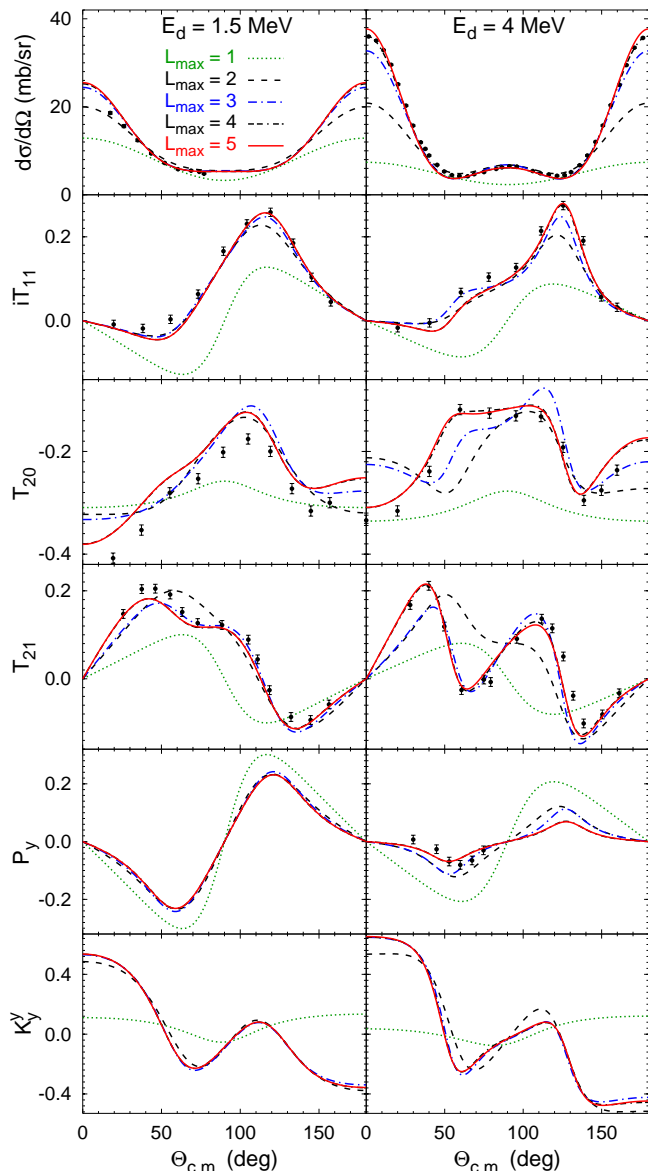


FIG. 8. (Color online) Observables of  $d + d \rightarrow n + {}^3\text{He}$  reaction at  $E_d = 1.5$  and 4 MeV. Results including initial and final states with two-cluster relative orbital angular momentum  $L \leq L_{\text{max}}$  are compared for  $L_{\text{max}}$  ranging from 1 to 5.  $L_{\text{max}} = 4$  and 5 results lie almost on top of each other. The experimental data are as in previous figures.

sor analyzing powers even at  $E_d = 1.5$  MeV. For other observables at this energy  $L_{\text{max}} = 3$  is sufficient while  $P_y$  is reasonably well converged with  $L_{\text{max}} = 2$ . It is interesting to note that  $L_{\text{max}} = 1$  results for most observables vary slowly with the energy while stronger energy dependence comes from  $L = 2, 3$ , and 4 partial waves. The above analysis partially explains sizable differences between our converged results and those of Ref. [25] obtained using the resonating group method (RGM) since the latter work included only  $L \leq 3$  states. Our AV18 results calculated with  $L_{\text{max}} = 3$  (not shown here) are qual-

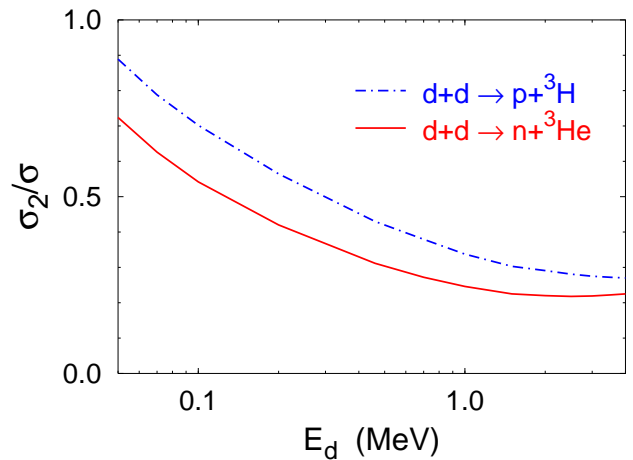


FIG. 9. (Color online) The quintet suppression factor  $\sigma_2/\sigma$  for  $d + d \rightarrow p + {}^3\text{H}$  and  $d + d \rightarrow n + {}^3\text{He}$  reactions as function of the deuteron lab energy.

itatively similar to the corresponding results of Ref. [25].

Finally we present results for the observables characterizing the spin correlations of the initial-state deuterons. We are not aware of the existence of the experimental data, but there are plans [26, 27] for future experiments involving the direct measurement of the so-called quintet suppression factor (QSF) defined as the ratio  $\sigma_2/\sigma$ , where  $\sigma_2$  is the cross section for the considered transfer reaction with the spins of the initial state deuterons being parallel, i.e., with the total spin being 2, and  $\sigma$  is the unpolarized (spin-averaged) cross section. As mentioned in the introduction, this observable is relevant for  $d-d$  fusion in hot plasma. Results obtained using INOY04 potential for  $E_d$  between 50 keV and 4 MeV are shown in Fig. 9. The QSF for the  $d + d \rightarrow n + {}^3\text{He}$  reaction is indeed smaller than for  $d + d \rightarrow p + {}^3\text{H}$ ; however, the difference is only about 20 - 25% in the whole considered regime. The energy dependence of the QSF is in both reactions similar: it is of the order of 0.25 above  $E_d = 2$  MeV but increases more rapidly as the energy decreases. Nevertheless, our QSF prediction are somehow smaller than the values obtained from  $R$ -matrix analysis and RGM [13]. This observable shows also strong dependence on the  $NN$  force model, e.g., the QSF values for the  $d + d \rightarrow n + {}^3\text{He}$  reaction at  $E_d = 3$  MeV predicted by AV18, N3LO, CD Bonn, CD Bonn +  $\Delta$ , and INOY04 models are 0.133, 0.159, 0.164, 0.185, and 0.219, respectively. Thus, the QSF correlates with both  $3N$  binding energy and  $P_D(d)$ , increasing when the former increases and/or the latter decreases.

In summary, we performed exact four-particle calculations of  $d + d \rightarrow p + {}^3\text{H}$  and  $d + d \rightarrow n + {}^3\text{He}$  reactions with several realistic  $NN$  potentials. Energy dependence of the differential cross section and spin observables was studied below three-body breakup threshold. Correlations of the predictions with  $3N$  binding energy and deuteron  $D$ -state probability  $P_D(d)$  were ob-

served. The INOY04 potential that fits both  ${}^3\text{He}$  and  ${}^3\text{H}$  experimental binding energies and has the smallest  $P_D(d) = 3.60\%$  among all realistic potentials, accounts well for the experimental data with only few discrepancies, e.g., the one in the deuteron tensor analyzing power

$T_{20}$ . Some data suggest that even smaller  $P_D(d)$  would be preferred. We also predict the quintet suppression factor in the  $d + d \rightarrow n + {}^3\text{He}$  reaction to be only up to 25% smaller than the one in  $d + d \rightarrow p + {}^3\text{H}$ ; the  $d$ - $d$  fusion with spin-aligned deuterons seems to be significantly suppressed at few MeV but not in the keV regime.

- 
- [1] A. Deltuva and A. C. Fonseca, Phys. Rev. C **75**, 014005 (2007).
- [2] A. Deltuva and A. C. Fonseca, Phys. Rev. C **76**, 021001(R) (2007).
- [3] P. Grassberger and W. Sandhas, Nucl. Phys. **B2**, 181 (1967); E. O. Alt, P. Grassberger, and W. Sandhas, JINR report No. E4-6688 (1972).
- [4] J. M. Blair, G. Freier, E. Lampi, W. Sleator, and J. H. Williams, Phys. Rev. **74**, 1599 (1948).
- [5] G. T. Hunter and H. T. Richards, Phys. Rev. **76**, 1445 (1949).
- [6] W. Grüebler, V. König, P. A. Schmelzbach, R. Risler, R. E. White, and P. Marmier, Nucl. Phys. **A193**, 129 (1972).
- [7] W. Grüebler, V. König, P. A. Schmelzbach, B. Jenny, and J. Vybiral, Nucl. Phys. **A369**, 381 (1981).
- [8] L. J. Dries, H. W. Clark, R. Detomo, and T. R. Donoghue, Phys. Lett. **80B**, 176 (1979).
- [9] R. A. Hardekopf, R. L. Walter, and T. B. Clegg, Phys. Rev. Lett. **28**, 760 (1972).
- [10] P. Lisowski, R. Walter, C. Busch, and T. Clegg, Nucl. Phys. **A242**, 298 (1975).
- [11] C. D. Roper, T. B. Clegg, J. D. Dunham, A. J. Mendez, W. Tornow, and R. L. Walter, Few-Body Syst. **47**, 177 (2010).
- [12] R. M. Kulsrud, H. P. Furth, E. J. Valeo, and M. Goldhaber, Phys. Rev. Lett. **49**, 1248 (1982).
- [13] H. M. Hofmann and D. Fick, Phys. Rev. Lett. **52**, 2038 (1984).
- [14] O. A. Yakubovsky, Yad. Fiz. **5**, 1312 (1967) [Sov. J. Nucl. Phys. **5**, 937 (1967)].
- [15] J. R. Taylor, Nuovo Cimento B **23**, 313 (1974); M. D. Semon and J. R. Taylor, Nuovo Cimento A **26**, 48 (1975).
- [16] A. Deltuva, A. C. Fonseca, and P. U. Sauer, Phys. Rev. C **71**, 054005 (2005); **72**, 054004 (2005).
- [17] A. Deltuva and A. C. Fonseca, Phys. Rev. Lett. **98**, 162502 (2007).
- [18] E. O. Alt and W. Sandhas, Phys. Rev. C **21**, 1733 (1980).
- [19] R. B. Wiringa, V. G. J. Stoks, and R. Schiavilla, Phys. Rev. C **51**, 38 (1995).
- [20] R. Machleidt, Phys. Rev. C **63**, 024001 (2001).
- [21] P. Doleschall, Phys. Rev. C **69**, 054001 (2004).
- [22] D. R. Entem and R. Machleidt, Phys. Rev. C **68**, 041001(R) (2003).
- [23] A. Deltuva, R. Machleidt, and P. U. Sauer, Phys. Rev. C **68**, 024005 (2003).
- [24] A. Deltuva, A. C. Fonseca, and P. U. Sauer, Phys. Lett. B **660**, 471 (2008).
- [25] H. M. Hofmann and G. M. Hale, Phys. Rev. C **77**, 044002 (2008).
- [26] H. Paetz gen. Schieck, private communication.
- [27] J.-P. Didelez, private communication.